PHOTONIC SENSORS / Vol. 6, No. 3, 2016: 279−288

Design and Optimization of Photonic Crystal Fiber for Liquid Sensing Applications

Md. Faizul Huq ARIF[1], Kawsar AHMED[1*], Sayed ASADUZZAMAN[1], and Md. Abul Kalam AZAD[2]

[1]*Department of Information and Communication Technology (ICT), Mawlana Bhashani Science and Technology University (MBSTU), Tangail-1902, Bangladesh*

[2]*Department of Material and Metallurgical Engineering (MME), Bangladesh University of Engineering and Technology University (BUET), Dhaka-1000, Bangladesh*

[*]Corresponding author: Kawsar AHMED E-mail: kawsar.ict@mbstu.ac.bd and kawsar_it08050@yahoo.com

Abstract: This paper proposes a hexagonal photonic crystal fiber (H-PCF) structure with high relative sensitivity for liquid sensing; in which both core and cladding are microstructures. Numerical investigation is carried out by employing the full vectorial finite element method (FEM). The analysis has been done in four stages of the proposed structure. The investigation shows that the proposed structure achieves higher relative sensitivity by increasing the diameter of the innermost ring air holes in the cladding. Moreover, placing a single channel instead of using a group of tiny channels increases the relative sensitivity effectively. Investigating the effects of different parameters, the optimized structure shows significantly higher relative sensitivity with a low confinement loss.

Keywords: Photonic crystal fiber (PCF); liquid sensor; microstructure core; sensitivity; confinement loss

Citation: Md. Faizul Huq ARIF, Kawsar AHMED, Sayed ASADUZZAMAN, and Md. Abul Kalam AZAD, "Design and Optimization of Photonic Crystal Fiber for Liquid Sensing Applications," *Photonic Sensors*, 2016, 6(3): 279–288.

1. Introduction

The field of fiber optics is no longer limited into telecommunication and medical science only; it has been developing in an incredible pace with large dimensions of applications. Fiber optic technologies have made a revolutionary change after the invention of photonic crystal fiber (PCF). PCF is a new class of optical fiber which is one of the recent inventions in the field of fiber optics. PCF can be used as a transmission media as well as optical functional devices. In contrast to the conventional optical fiber, PCFs have additional design features, such as air-hole diameter, pitch size, and number of rings, which offer to overcome many limitations of conventional fiber.

Due to the well-known advantages, such as enhanced design freedom, low cost, short-time detection, small size, robustness, and high sensitivity and flexibility PCFs have received considerable attention in developing optodevices and sensors. Photonic crystal fibers (PCFs) have been attracted a great deal of attention for its incredible performance and large variety of applications. PCF can be used as filters [1], switches [2, 3], electro-optical modulators [4, 5], polarization converters [6], sensors [7−17], etc. PCF based sensors are smart applications in fiber optic technology which have been

Received: 17 February 2016 / Revised: 6 June 2016

DOI: 10.1007/s13320-016-0323-y
Article type: Regular

investigating and developing since last decade. A wide range of sensing applications of PCF are available, such as temperature sensors [7], refractive index (R.I) sensors [8], chemical sensors [9], mechanical sensors [10], pressure sensors [11], gas sensors [12,13], stress sensors [14], pH sensors [15], liquid sensors [16], biosensors [17], and so on. An ideal candidate of optical sensors is index guiding PCF. The sensing mechanism of index guiding PCF is evanescent interaction between the optical field and the analyte to be sensed. The evanescent field based PCF sensors have been developing rapidly for chemical and biomedical applications due to their attractive features.

Highly sensitive chemical (liquid and gas) sensors are playing an important role in the industrial processes [18] especially for detecting toxic and flammable chemicals (e.g., toxic gasses or liquids) to overcome the safety issues. So it has become one of the key challenges to enhance the performance of liquid and gas sensors. In recent years, researchers are keeping much interest on the development of photonic crystal fiber (PCF) based sensors for environmental and safety monitoring [19, 20] issues. Photonic crystal fiber based liquid and gas sensors through the evanescent field show excellent performance in terms of sensitivity, because core of the PCF directly interacts with the material to be analyzed.

PCF technologies allow for the accurate tuning of fiber through changing the air hole shape, size, and their position. A wide variety of PCF based sensing techniques have been reported by changing different geometric parameters of the PCF to gain sensitivity at a maximum and confinement loss at a minimum satisfactory level in liquid and gas sensing applications. J. Park *et al*. [21] enhanced relative sensitivity for chemical sensing, using a hexagonal PCF with a hollow high indexed ring defect. In the hollow core PCF, the direct interaction between light and the analyte in the hollow channel is higher than the index-guided PCFs. Recently, the idea of filling core or cladding holes with various liquids or gases has been attracted much to the researchers. Cordeiro *et al*. [22] proposed a microstructure core PCF infiltrated with liquid analyte which enhanced the evanescent field. This concept introduced the sensing potentiality with infiltrated microstructure core. PCF of microstructure core offers to sense low indexed material because of the highly interaction of evanescent fields with the analyst to be sensed. A large number of published papers investigated and enhanced the performance of PCF based gas and liquid sensors with microstructure core [23−28].

In recent study, higher sensitivity and lower confinement loss of microstructure core PCF for liquid sensing have been attempted by using octagonal cladding structure [24, 25]. Reference [25] suggested 5-ring octagonal PCF for higher sensitivity and lower confinement loss; but in practical manufacturing octagonal structure requires extra more capillaries than the hexagonal structure. Keeping large number of capillaries will make high cost to fabricate. In this point of view, liquid sensing using a single infiltrated channel may also reduce the complexity of the core. To the best of our knowledge, no studies have been done in analyzing the sensitivity performance of PCF with a liquid filled core of a single channel.

In this research work, we have proposed and optimized simple evanescent hexagonal structure of PCF (H-PCF) with microstructure core and cladding for liquid sensing, which shows high relative sensitivity as well as low confinement loss. We have also explained the effect of single infiltrated channel replacing the microstructure core by proposing another structure of PCF, which achieved more enhancements of relative sensitivity and simplicity in design. We have not used any defect around the hollow core; though one of the previous articles [21] enhanced relative sensitivity by using a ring defect around the core. The relative sensitivity and confinement loss against different liquids (water, ethanol, and benzyne) have been investigated and

compared. Although we have chosen water, ethanol, and benzyne as the targeted chemical species for characterization of our structures but these structures and the mechanism can be applied for all fluids and gases based on the absorption line of the targeted sample.

2. Design principle

Figure 1 shows the transverse cross sectional view of the four stages of our proposed PCF structure. The proposed PCF contains only four layers of air holes in the cladding. The distance between center and center of two adjacent air holes (pitch distance) has been denoted by Λ. The diameters of air holes in the innermost ring, second ring, third ring, and outermost ring are d_1, d_2, d_3, and d_4, respectively. In PCF_1, the diameter of all air holes is equal, where $d_1=d_2=d_3=d_4$.

In our numerical investigation, we found that the outermost ring holes diameter has greater impact on the confinement loss, and then we have come into PCF_2. In PCF_2, $d_1=d_2=d_3<d_4$. Another result of our numerical investigation shows that larger diameter of the innermost ring holes enhances the sensitivity and we have turned into PCF_3. In PCF_3, optimized values of air holes diameter have been kept as $d_2=d_3<d_1=d_4$. However, we have turned into PCF_4 and achieved higher sensitivity by replacing the group of tiny holes with a single hollow core filled with same analyte to be detected. The hollow core area is same as the area covered by supplementary tiny holes. In the PCF_1, PCF_2, and PCF_3, the core is designed with some tiny holes in circular form which are filled with various liquid samples: water, ethanol, and benzyne for this study. These supplementary core holes are arranged with the hole to hole pitch distance denoted by a. Figure 2 visualizes the enlarged view of core of PCF_1, PCF_2, PCF_3, and the replacement of hollow channel instead of using a group of tiny channels in PCF_4. Diameter of the hollow channel is D_2=1.70 μm, which is same as the diameter of the region of supplementary holes in the core ($D_1=D_2$).

Figure 3 shows the computational region of the proposed PCF_3 and PCF_4, which is divided into homogeneous triangular pieces forming a mesh. Each of the PCFs has two orthogonal sides of the computational region which are assigned with two artificial boundary conditions: perfect electric conductor (PEC) and perfect magnetic conductor (PMC). Perfectly matched layer (PML) is used as a boundary condition. Thickness of the PML is fixed to 10% of the radius of the proposed PCFs for efficient calculation of confinement loss [29].

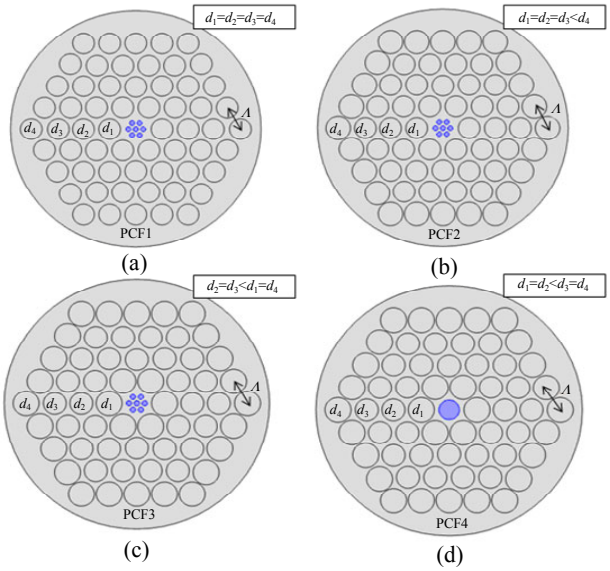

Fig. 1 Transverse cross sectional view of (a) PCF_1, (b) PCF_2, (c) PCF_3, and (d) PCF_4.

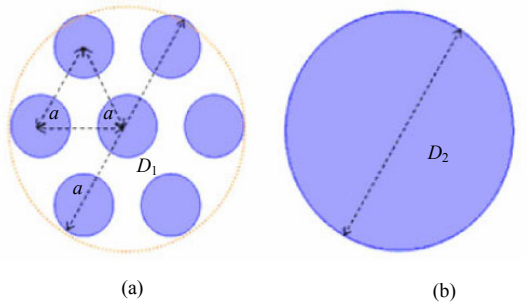

Fig. 2 Enlarged view of core region of (a) PCF_1, PCF_2, and PCF_3 and (b) PCF_4.

3. Principles of operation

PCFs act as a waveguide, and in this wave guide,

and the targeted analyte and light interact with each other. We have analyzed the evanescent field distribution of the proposed PCFs. Using the finite element method (FEM), the properties of propagating mode of the proposed PCFs is numerically investigated. We have considered circular perfectly matched layer (PML) as a boundary condition. The cross sections of the proposed PCFs are divided into homogeneous triangular subspaces using mesh analysis shown in Fig. 3. The liquid filled air holes' region is then divided into many sub-domains which are either triangular or quadrilateral in shape. Using FEM, Maxwell's equations are solved by accounting neighboring subspaces. As the wave propagates through z direction, the modal analysis has been performed in the x-y plane of the PCF structure. The following vectorial wave equation can be derived from the Maxwell's equation [30].

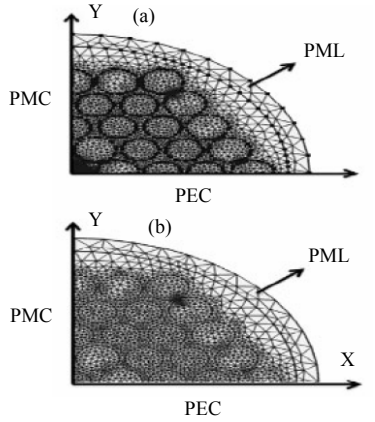

Fig. 3 FEM meshes and boundary conditions for computation of (a) PCF_3 and (b) PCF_4.

$$\nabla \times (\mathbf{S}^{-1}\nabla \times E) - k_0{}^2 n^2 \mathbf{S}E = 0 \tag{1}$$

where $\mathbf{S}$ represents the PML matrix of 3×3 and $\mathbf{S}^{-1}$ is the inverse of $\mathbf{S}$ matrix. The symbol E denotes the electric field vector, n is the refractive index of the domain, K_0 is the wave number in free space, and λ is the operating wavelength. The propagating constant β is represented by the following equation.

$$\beta = n_{\text{eff}} K_0 \tag{2}$$

Due to the finite number of air holes in the cladding part, there may cause leakage of light. The leakage of light from core to exterior materials results in confinement loss (dB/m) which can be obtained from the imaginary part of n_{eff} by using the following equation [24].

$$L_c = 8.868 \times K_0 I_m[n_{\text{eff}}]\,(\text{dB/m}). \tag{3}$$

However, this leakage of light energy can be omitted by using an infinite number of air holes. But in practical, the number of air holes is finite.

The relative sensitivity coefficient measures the interaction between the light and the analyte to be sensed. This interaction is measured through the absorption coefficient at a particular wavelength. According to the Beer-Lambert law, light is attenuated by the intensity of absorption of evanescent wave [31]

$$I(\lambda) = I_0(\lambda)\exp[-r\alpha_m l_c] \tag{4}$$

The absorbance of the sample to be detected is defined by the following equation [27]:

$$A = \lg\left(\frac{I}{I_0}\right) = r\alpha_m l_c \tag{5}$$

where I and I_0 are the input and output intensities, respectively, and c is the concentration of absorbing material. The length of the channel is l. The function of absorption coefficient is $\alpha_m(\lambda)$ and r is the relative sensitivity coefficient, which can be defined by the following equation [22]

$$r = \frac{n_r}{n_{\text{eff}}} f \tag{6}$$

where n_r refers to the refractive index of the sample to be sensed, and n_{eff} is the effective index of the guided mode. f is the fraction of total power located in the core, and it is also known as a power distribution function [28] by using Poynting's theorem which can be expressed as the following equation:

$$f = \frac{\int_{\text{holes}} \text{Re}(E_x H_y - E_y H_x)dxdy}{\int_{\text{total}} \text{Re}(E_x H_y - E_y H_x)dxdy} \tag{7}$$

where E_x and H_x are transverse electric field and

magnetic field respectively; E_y and H_x are longitudinal electric field and magnetic field respectively. Using FEM the mode field pattern and effective index are obtained. During the simulation, we have considered the material dispersion of silica background using the Sellmeier equation [32].

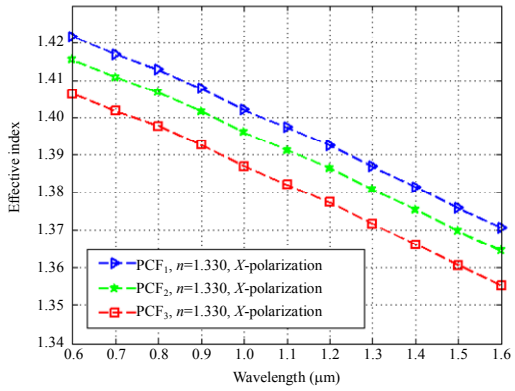

Fig. 4 Effective index curves of the fundamental mode for the *X*-polarization with Λ=2.4 μm, d=0.45 μm. PCF_1: $d_1=d_2=d_3=d_4$=1.9 μm; PCF_2: $d_1=d_2=d_3$=1.9 μm and d_4=2.15 μm; PCF_3: $d_2=d_3$=1.9 μm and $d_1=d_4$=2.15 μm.

4. Results and discussion

This section describes the numerical analysis of propagation characteristics in fundamental mode and some higher order modes of the proposed PCFs. Three liquid analytes, water, ethanol, and benzyne, have been selected for filling the supplementary core holes. Here, it has been considered *X*-polarization of fundamental mode for this investigation. The initial analysis has been performed by assuming the geometric parameters of PCF_1: $d_1=d_2=d_3=d_4$=1.9 μm; PCF_2: $d_1=d_2=d_3$=1.9 μm and d_4=2.15 μm; PCF_3: $d_2=d_3$=1.9 μm and $d_1=d_4$=2.15 μm. The supplementary holes pitch ratio is d/a=0.70. The center-to-center air holes distance is Λ=2.4 μm at the cladding, which has been kept fixed for all of the proposed PCFs. The simulation has been performed at a wide range of wavelength from 0.6 μm to 1.6 μm. The simulation process has been down using COMSOL Multiphysics 4.2 by selecting a fine mode of mesh size. The convergence error seems very low of proposed PCFs about 3.55×10^{-5}% and 3.50×10^{-5} % for PCF_3 and PCF_4, respectively.

Initially, Fig. 4 shows the effective index profile of PCF_1, PCF_2, and PCF_3. It is clear from Fig. 4 that the effective indices decrease linearly with an increase in wavelength. It can be evidently seen that the PCF_1 shows higher effective index values among the first three proposed PCFs.

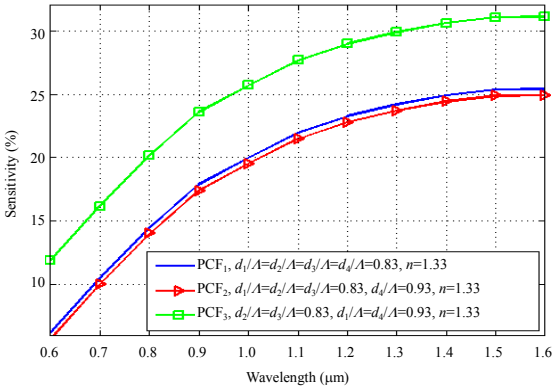

(a)

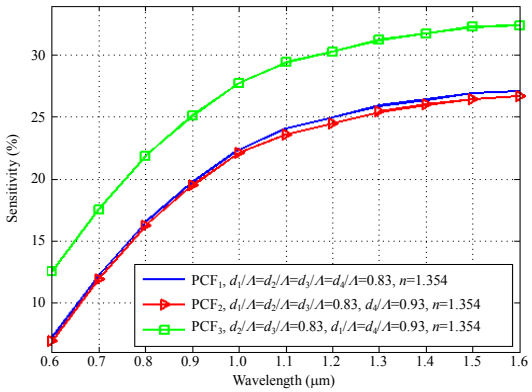

(b)

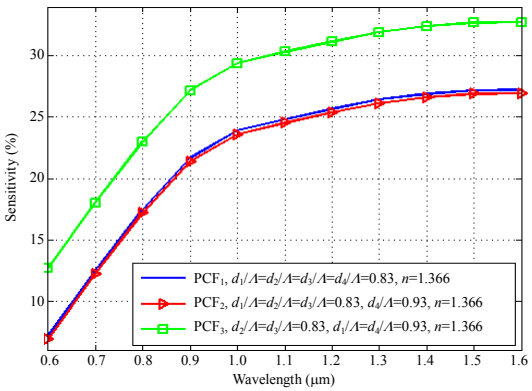

(c)

Fig. 5 Comparison of the relative sensitivity of PCF_1, PCF_2, and PCF_3 for (a) water, (b) ethanol, and (c) benzyne, where Λ=2.4 μm, d=0.45 μm. PCF_1: $d_1=d_2=d_3=d_4$=1.9 μm; PCF_2: $d_1=d_2=d_3$=1.9 μm, and d_4=2.15 μm; PCF_3: $d_2=d_3$=1.9 μm, and $d_1=d_4$=2.15 μm.

Figure 5 presents the relative sensitivity curves of PCF_1, PCF_2, and PCF_3 for the three analytes as a function of wavelength. There is no significant change in sensitivity for PCF_1 and PCF_2 in all wavelengths. Therefore, no significant impacts on sensitivity have been observed with increasing diameters of outer rings holes. However, the relative sensitivity of PCF_3 is greatly enhanced. At the wavelength λ=1.33 μm, for water, ethanol, and benzyne, the calculated sensitivity of PCF_3 is 30%, 32.5%, and 33.67%, respectively and the confinement loss is 3.25×10^{-10} dB/m, 2.95×10^{-10} dB/m, and 2.31×10^{-10} dB/m, respectively. The reason behind the enhanced sensitivity of PCF_3 is that the increment of the inner ring holes diameter leads them closer to the core area and the fraction of evanescent field penetrates to the holes increase and relative sensitivity of the PCF_3 increases consequently. It is also clear that higher index material shows higher relative sensitivity.

Figure 6 illustrates the relative sensitivity performance of PCF_3 varying the diameter (d) of the supplementary holes in the core region. According to this inquiry, the sensitivity increases with the increment of the diameter of supplementary holes. From Fig. 6, we have found the highest relative sensitivity when d=0.55 μm. For this value of the supplementary holes diameter, PCF_3 shows relative sensitivity 48.50% and 47.78%, and confinement loss 1.28×10^{-10} dB/m and 5.37×10^{-11} dB/m for ethanol and water, respectively, at the wavelength λ=1.33 μm.

To achieve much more relative sensitivity, we have proposed PCF_4 replacing a single hollow channel instead of using supplementary tiny holes. In PCF_4, the diameter of the hollow channel is D_2=1.70 μm. Figure 7 depicts the comparative performance of sensitivity of the last two proposed PCFs: PCF_3 and PCF_4 for all types of analytes used in this study. According to Fig. 7, PCF_4 shows great enhancement of relative sensitivity. At the wavelength λ=1.33 μm, PCF_4 exhibits the relative sensitivity 50%, 55.83%, and 59.07%, confinement loss 4.25×10^{-10} dB/m, 8.72×10^{-10} dB/m, and 2.56×10^{-10} dB/m for water, ethanol, and benzyne, respectively.

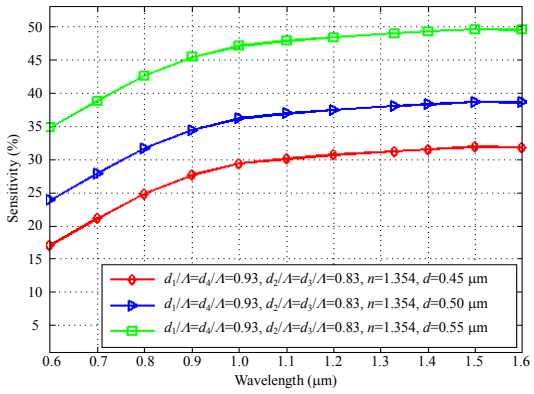

(a)

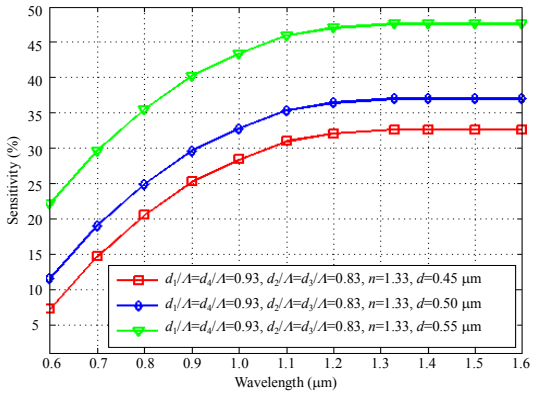

(b)

Fig. 6 Comparison of relative sensitivity of PCF_3 as a function of operating wavelength for (a) ethanol (b) water; where d=0.45 μm, d=0.50 μm, d=0.55 μm, and rest of the parameters are fixed as before.

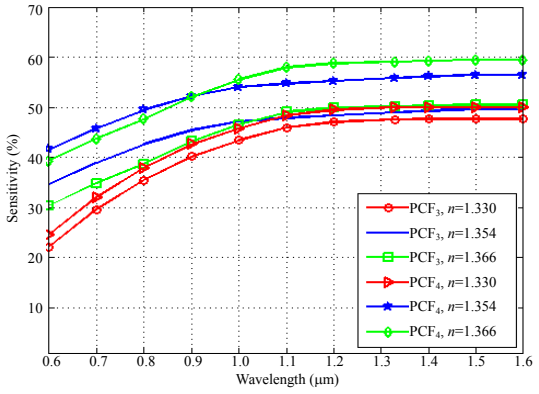

Fig. 7 Relative sensitivity versus wavelength for PCF_3 and PCF_4 with Λ=2.4 μm, d=0.55μm, D_2=1.70 μm, d_2=d_3=1.9 μm, and d_1=d_4=2.15 μm.

Figure 8 presents the confinement loss curves of PCF_3 and PCF_4. With the investigation of Fig. 8, it can be seen that PCF_4 exhibits better performance in terms of confinement loss for all types of analytes used in this study. Therefore, it can be said that the light mode is more confined in the core region for the proposed PCF_4 compared with the first three proposed PCF structures. This may be linked to the fact that the electromagnetic interaction between the propagated light and analyte is higher which causes an increase in relative sensitivity. In addition, from Fig. 8, it can be found that lower confinement losses are achieved with higher indexed liquids. According to the overall discussion, PCF_4 shows higher sensitivity and lower confinement loss than PCF_3.

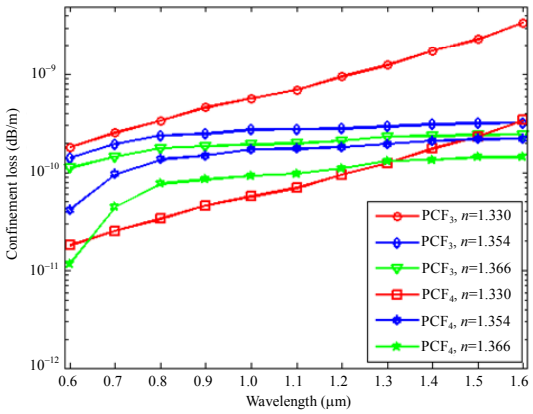

Fig. 8 Confinement loss versus wavelength for PCF_3 and PCF_4 with Λ=2.4 μm, d=0.55 μm, D_2=1.70 μm, d_2=d_3=1.9 μm, and d_1= d_4=2.15 μm.

In order to support the numerical results reported in the figures, the electric field distribution of the proposed PCF_3 and PCF_4 has been illustrated in Fig. 9, where the operating wavelength is set to λ=1.33 μm and the core holes are filled with ethanol. It can be clearly seen that the fundamental mode of our optimized PCFs (PCF_3 and PCF_4) is tightly confined in the core region.

From the overall discussion, we have found that our designed structures show better performance in relative sensitivity with more design simplicity than the prior structures [24, 25] for liquid sensing. Table 1 shows the comparative performance analysis between prior PCFs and proposed PCFs for liquid sensing at the wavelength λ=1.33 μm. Tables 2 and 3 represent the sensitivity dependency on diameters and global parameters variations, respectively. Although, diameters are varied after fabrication but it has no global effects on result of the proposed structure.

Table 1 Comparison between proposed PCFs and prior PCFs for liquid sensing applications at λ=1.33 μm.

PCFs	Sensitivity (%)		Structural shape description
	Ethanol (n=1.354)	Benzyne (n=1.366)	
Ref. [24]	21.55	22.50	Octagonal shape: 3 rings
Ref. [25]	46.87	47.35	Octagonal shape: 5 rings
Proposed PCF_3	48.50	50.08	Hexagonal shape: 4 rings
Proposed PCF_4	55.83	59.07	Hexagonal shape: 4 rings

Table 2 Comparison of sensitivity for optimum design parameters and also for fiber's global diameter variations of order ±1%–±3% around the optimum value at λ=1.33 μm.

Only diameter variations (%)	Relative sensitivity (%)	
	PCF_3	PCF_4
−3	44.05	48.46
−1	46.98	53.29
Optimum	48.50	55.83
+1	50.09	57.84
+3	53.31	61.13

Through the experimental point of view, the fabrication feasibility of the proposed PCFs is an important part. It seems that the fabrication process of the micro cored region may not be easy. However, due to the technological advancement, the fabrication of our recommended PCFs is possible. Micro core must be filled with the analyte without damaging the fiber's integrity. Now, several techniques are available for filling the PCF holes with analytes. Huang *et al*. [33] proposed a unique method for selectively filling the all cladding holes as well as micro core holes. The fabrication of PCF with liquid filled core or cladding can be accomplished with the same method [34, 35]. Now, applying the sol-gel technique [36] any kind of complexity of fabrication of microstructure optical fiber can be removed. In this regard, our proposed

PCF structures can be fabricated with the currently available nanotechnology. Selective filling technique [37] can be used for fill the analytes (gas or liquids) at the core.

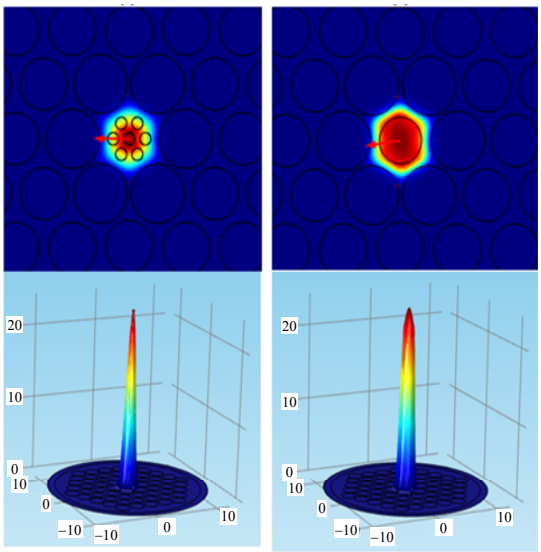

(a) (b)

Fig. 9 2d and 3d views of modal Intensity distribution of (a) PCF_3 and (b) PCF_4 for *X*-polarized mode at the wavelength λ=1.33 μm where $n_{eff\text{-}x}$=1.3753 for PCF_3 and $n_{eff\text{-}x}$=1.3455 for PCF_4.

Table 3 Comparison of sensitivity for optimum design parameters and also for fiber's global parameters variations of order ±1%–±3% around the optimum value at λ=1.33 μm.

All parameters variation (%)	Relative sensitivity (%)	
	PCF3	PCF4
−3	48.72	56.46
−1	48.58	56.03
Optimum	48.50	55.83
+1	48.41	55.53
+3	48.23	55.03

5. Conclusions

In this study, the enhancement of the performance of the PCF based liquid sensor has been done by our recommended two structures of PCF, which are based on microstructure core and hollow core, and infiltrated with the liquid to be sensed. All of the proposed structures with microstructure core and liquid core have better guiding capability and the manufacturing of this type of structure is possible with the current nanofabrication techniques [34−38]. Our proposed PCF provided higher relative sensitivity with tighter confinement of optical field than the prior PCF structures. Therefore, our proposed PCFs can successfully overcome the critical trade-off between confinement loss and sensitivity, and it is assumed that our proposed structures of PCF offer great potentiality for toxic chemical and gas detection in industrial safety purposes.

References

[1] M. Arjmand and R. Talebzadeh, "Optical filter based on photonic crystal resonant cavity," *Optoelectronics and Advanced Materials-Rapid Communications*, 2015, 9(1−2): 32−35.

[2] K. Fasihi, "High-contrast all-optical controllable switching and routing in nonlinear photonic crystals," *Journal of Lightwave Technology*, 2014, 32(18): 3126−3131.

[3] K. Cui, Q. Zhao, X. Feng, Y. Huang, Y. Li, D. Wang, *et al*., "Thermo-optic switch based on transmission-dip shifting in a double-slot photonic crystal waveguide," *Applied Physics Letters*, 2012, 100(20): 201102-1−201102-4.

[4] J. M. Brosi, C. Koos, L. C. Andreani, M. Waldow, J. Leuthold, and W. Freude, "High-speed low-voltage electro-optic modulator with a polymer-infiltrated silicon photonic crystal waveguide," *Optics Express*, 2008, 16(6): 4177−4191.

[5] Y. Gao, R. J. Shiue, X. Gan, L. Li, C. Peng, I. Meric, *et al*., "High-speed electro-optic modulator integrated with graphene-boron nitride heterostructure and photonic crystal nanocavity," *Nano Letters*, 2015, 15(3): 2001−2005.

[6] H. Xuan, J. Ma, W. Jin, and W. Jin, "Polarization converters in highly birefringent microfibers," *Optics Express*, 2014, 22(3): 3648−3660.

[7] Y. H. Chang, Y. Y. Jhu, and C. J. Wu, "Temperature dependence of defect mode in a defective photonic crystal," *Optics Communications*, 2012, 285(6): 1501−1504.

[8] Y. Liu and H. W. M. Salemink, "All-optical on-chip sensor for high refractive index sensing in photonic crystals," *Europhysics Letters*, 2014, 107(3):

1160−1170.

[9] S. Zheng, Y. Zhu, and S. Krishnaswamy, "Nanofilm-coated photonic crystal fiber long-period gratings with modal transition for high chemical sensitivity and selectivity," *Proc. SPIE*, 2012, 8346(14): 1844−1864.

[10] C. Lee and J. Thillaigovindan, "Optical nanomechanical sensor using a silicon photonic crystal cantilever embedded with a nanocavity resonator," *Applied Optics*, 2009, 48(10): 1797−1803

[11] S. Olyaee and A. A. Dehghani, "Ultrasensitive pressure sensor based on point defect resonant cavity in photonic crystal," *Sensor Letters*, 2013, 11(10): 1854−1859.

[12] Y. N. Zhang, Y. Zhao, and Q. Wang, "Multi-component gas sensing based on slotted photonic crystal waveguide with liquid infiltration," *Sensors and Actuators B: Chemical*, 2013, 184(8): 179−188.

[13] M. Morshed, M. F. H. Arif, S. Asaduzzaman, and K. Ahmed, "Design and characterization of photonic crystal fiber for sensing applications," *European Scientific Journal*, 2015, 11(12): 228−235.

[14] T. W. Lu and P. T. Lee, "Ultra-high sensitivity optical stress sensor based on double-layered photonic crystal microcavity," *Optics Express*, 2009, 17(3): 1518−1526.

[15] P. Hu, X. Dong, W. C. Wong, L. H. Chen, K. Ni, and C. C. Chan, "Photonic crystal fiber interferometric pH sensor based on polyvinyl alcohol/polyacrylic acid hydrogel coating," *Applied Optics*, 2015, 54(10): 2647−2652.

[16] W. C. Lai, S. Chakravarty, Y. Zou, and R. T. Chen, "Multiplexed detection of xylene and trichloroethylene in water by photonic crystal absorption spectroscopy," *Optics Letters*, 2013, 38(19): 3799−3802.

[17] E. K. Akowuah, T. Gorman, H. Ademgil, S. Haxha, G. K. Robinson, and J. V. Oliver, "Numerical analysis of a photonic crystal fiber for biosensing applications," *IEEE Journal of Quantum Electronics*, 2012, 48(11): 1403−1410.

[18] M. B. Pushkarsky, M. E. Webber, O. Baghdassarian, L. R. Narasimhan, and C. K. N. Patel, "Laser-based photoacoustic ammonia sensors for industrial applications," *Applied Physics B*, 2002, 75(2-3): 391-396.

[19] G. Whitenett, G. Stewart, K. Atherton, B. Culshaw, and W. Johnstone, "Optical fibre instrumentation for environmental monitoring applications," *Journal of Optics A: Pure and Applied Optics*, 2003, 5(5): S140−S145.

[20] J. P. Carvalho, H. Lehmann, H. Bartelt, F. Magalhaes, R. Amezcua-Correa, J. L. Santos, *et al*., "Remote system for detection of low-levels of methane based on photonic crystal fibres and wavelength modulation spectroscopy," *Journal of Sensors*, 2009, 2009(2): 1−10.

[21] J. Park, S. Lee, S. Kim, and K. Oh, "Enhancement of chemical sensing capability in a photonic crystal fiber with a hollow high index ring defect at the center," *Optics Express*, 2011, 19(3): 1921−1929.

[22] C. M. Cordeiro, M. A. Franco, G. Chesini, E. C. Barretto, R. Lwin, C. B. Cruz, *et al*., "Microstructured-core optical fibre for evanescent sensing applications," *Optics Express*, 2006, 14(26): 13056−13066.

[23] M. Morshed, H. M. Imarn, T. K. Roy, M. S. Uddinand, and S. A. Razzak, "Microstructure core photonic crystal fiber for gas sensing applications," *Applied Optics*, 2015, 54(29): 8637−8643.

[24] H. Ademgil, "Highly sensitive octagonal photonic crystal fiber based sensor," *Optik−International Journal for Light and Electron Optics*, 2014, 125(20): 6274−6278.

[25] K. Ahmed and M. Morshed, "Design and numerical analysis of microstructured-core octagonal photonic crystal fiber for sensing applications," *Sensing and Bio-Sensing Research*, 2016, 7: 1−6.

[26] S. Asaduzzaman, K. Ahmed, M. F. H. Arif, and M. Morshed, "Proposal of simple structure photonic crystal fiber for lower indexed chemical sensing," in *18th International Conference on Computer and Information Technology*, MIST, Bangladesh, 2015.

[27] S. Asaduzzaman, K. Ahmed, and M. F. H. Arif, "Numerical analysis of O-PCF structure for sensing applications with high relative sensitivity," in *2nd International Conference on Electrical Information and Communication Technology*, KUET, Bangladesh, 2015.

[28] S. Asaduzzaman, K. Ahmed, M., M. F. H. Arif, and M. Morshed, "Application of microarray-core based modified photonic crystal fiber in chemical sensing," in *International Conference on Electrical and Electronic Engineering*, RUET, Bangladesh, 2015.

[29] M. Morshed, M. I. Hasan, and S. M. A. Razzak, "Enhancement of the sensitivity of gas sensor based on microstructure optical fiber," *Photonic Sensors*, 2015, 5(4): 312−320.

[30] S. Selleri, L. Vincetti, A. Cucinotta, and M. Zoboli, "Complex FEM modal solver of optical waveguides with PML boundary conditions," *Optical and Quantum Electronics*, 2001, *33*(4−5): 359−371.

[31] B. Q. Wu, Y. Lu, C. J. Hao, L. C. Duan, N. N. Luan, Z. Q. Zhao, *et al*., "December. hollow-core photonic crystal fiber based on C2H2 and NH3 gas sensor," *Applied Mechanics and Materials*, 2013, 411: 1577−1580.

[32] G. Ghosh, "Sellmeier coefficients and dispersion of

thermo-optic coefficients for some optical glasses," *Applied Optics*, 1997, 36(7): 1540−1546.

[33] Y. Huang, Y. Xu, and A. Yariv, "Fabrication of functional microstructured optical fibers through a selective-filling technique," *Applied Physics Letters*, 2004, 85(22): 5182−5184.

[34] M. Luo, Y. G. Liu, Z. Wang, T. Han, Z. Wu, J. Guo, *et al*., "Twin-resonance-coupling and high sensitivity sensing characteristics of a selectively fluid-filled microstructured optical fiber," *Optics Express*, 2013, 21(25): 30911−30917.

[35] R. M. Gerosa, D. H. Spadoti, C. J. de Matos, L. D. S. Menezes, and M. A. Franco, "Efficient and short-range light coupling to index-matched liquid-filled hole in a solid-core photonic crystal fiber," *Optics Express*, 2011, 19(24): 24687−24698.

[36] R. T. Bise and D. J. Trevor, "Sol-gel derived microstructured fiber: fabrication and characterization," in *Optical Fiber Communications Conference*, Anaheim, U.S.A., 2005.

[37] Y. Huang, Y. Xu, and A. Yariv, "Fabrication of functional microstructured optical fibers through a selective-filling technique," *Applied Physics Letters*, 2004, 85(22): 5182–5184.

[38] F. M. Cox, A. Argyros, and M. C. J. Large, "Liquid-filled hollow core microstructured polymer optical fiber," *Optics Express*, 2006, 14(9): 4135−4140.